CHALMERS
UNIVERSITY OF TECHNOLOGY

Quality of Transmission Aware Optical Networking Using Enhanced Gaussian Noise Model

Citation for the original published paper (version of record):
Rabbani, H., Beygi, L., Ghoshooni, S. et al (2019). Quality of Transmission Aware Optical Networking Using Enhanced Gaussian Noise Model. Journal of Lightwave Technology, 37(3): 831-838. http://dx.doi.org/10.1109/JLT.2018.2881607

(article starts on next page)

Quality of Transmission Aware Optical Networking using Enhanced Gaussian Noise Model

Hami Rabbani, Lotfollah Beygi, Saeedeh Ghoshooni, Hamed Rabbani, and Erik Agrell, *Fellow, IEEE*

***Abstract*—We present a new joint routing, wavelength, and power allocation method for optical network planning. The introduced gradient-based convex optimization approach has a lower computational complexity, compared to common linear programming techniques, suitable for both static as well as time-critical dynamic network planning with fast convergence requirement. The proposed scheme takes physical-layer impairments into account, using the enhanced Gaussian noise nonlinear model. In contrast to methods exploiting the theoretical full link spectrum utilization assumption (fully occupied fiber-optic C-band spectrum), we focus on maximizing the network achievable rate (AR) and minimum signal-to-noise ratio (SNR) margin of networks with partial spectrum utilization in their links, relevant to the majority of empirical metro network scenarios.**

According to numerical results, the network achievable rate can be improved around 17% by performing power optimization over the individual launch power of network lightpaths compared to optimizing a single flat (equal) launch power for all the lightpaths. Moreover, the minimum SNR margin of the simulated network is improved by about 2.3 dB. Finally, it is observed that maximizing the network minimum SNR margin needs the launch power of each lightpath to be proportional to the total nonlinear interference noise efficiency influencing the lightpath.

***Index Terms*—Enhanced Gaussian noise model, routing and wavelength assignment, power allocation, coherent transmission, non-linear effects, optical network optimization, network planning.**

I. Introduction

THE tremendous growth in the demand for high data rates in optical networks makes efficient utilization of available resources in these networks, such as fiber-optic spectrum and transceiver optical powers, indispensable [1]. To come up with an efficient resource-utilization network design, the three main steps of network planning, namely routing, wavelength assignment (RWA), and power allocation of lightpaths for a given network traffic matrix, need to be optimized jointly. The exploited optimization technique is performed subject to fulfilling the required quality of transmission (QoT) for each lightpath. The most overriding factor restricting the lightpath QoT apart from added noise by optical amplifiers is the nonlinear Kerr effect of fiber-opitc links [2], [3]. A counterpart of RWA introduced in wavelength division multiplexing (WDM) systems is routing and spectrum assignment (RSA) for elastic optical networks, providing higher flexibility in fiber-optic spectrum utilization but demanding higher computational complexity. Three routing algorithms, shortest path, simple congestion aware, and weighted congestion aware-routing, were proposed in [4] using Dijkstra's algorithm on a graph weighted proportionally to the spectrum occupation of the links. To minimize the number of sub-carriers in an elastic optical network, different routing methods were introduced in [5]–[8] using mixed integer linear programming (MILP). RWA can be applied in static or dynamic network planning, i.e., predetermined connection requests given by a fixed traffic matrix or dynamic connection requests arriving and terminating based on a stochastic process. In transparently routed wavelength optical networks, lightpaths between different source and destination pairs experience different nonlinear signal distortion due to traveling different distances and being exposed to different numbers of WDM neighbor channels.

To analytically evaluate achievable transmission rates and QoTs of fiber-optic links, many research works have been devoted to extracting channel models both in the time [9], [10] and frequency [11]–[13] domains. The Gaussian noise (GN) model was derived based on the assumption that the transmitted signal in a link gets Gaussian distribution [12], leading to overestimate of the nonlinear interference noise (NLIN) variance. Mecozzi et al. first addressed a modulation-format dependent time-domain model [9], assuming only the dominant nonlinear terms of cross-channel interference (XCI), known as cross-phase modulation (XPM) terms. Later, this time-domain model was studied comprehensively in [10] and compared with the GN model to address the discrepancy between these two models [14]. Following the same approach as [10], the authors of [12] added correction terms to the GN model, taking into account the self-channel interference (SCI), all XCI terms, and multi-channel interference (MCI) terms, giving rise to an enhanced Gaussian noise (EGN) model. The evaluation of achievable rate (AR) in nonlinear WDM systems with an arbitrary modulation format was investigated in [15].

Conservative optical network planning schemes are performed by assuring the QoT of the worst lighpath (with the largest length) to be above a certain minimum value [16]–[18] and considering a fully utilized spectrum in all the network links [19], while in most empirical optical network scenarios the links spectrum are utilized partially. Recently, exploiting the GN model [11], [20]–[23] has opened up a new horizon in optimizing routing, wavelength assignment, modulation level, channel coding, and power allocation in the planning of coherent polarization-multiplexed (PM) optical networks [4], [19], [24]–[26] to maximize the minimum received signal-to-noise ratio (SNR) or the network's total AR. Power optimization is performed considering either a single flat (equal) launch power over all lightpaths [19] or individual different power values for different lightpaths in the network [26]. The first case gives rise to a one-dimensional optimization problem, whereas the

Hami Rabbani, Lotfollah Beygi, and Saeedeh Ghoshooni are with the EE Dept. of K. N. Toosi University of Technology. Hamed Rabbani is with the Sina Innovative Communications Systems corporation. Erik Agrell is with the Dept. of Electrical Engineering, Chalmers University of Technology, Sweden. E-mail: hami.rabani87@gmail.com, beygi@kntu.ac.ir, Saeedeh.ghoshooni@email.kntu.ac.ir, hamedrabbani@yahoo.com, and agrell@chalmers.se

second case will be referred to as multidimensional power optimization. In [26], the authors have introduced a disjoint wavelength assignment (WA) and power allocation scheme, where the exploited WA method does not account for physical-layer impairments (mainly a congestion-aware approach [4]). We have exploited the same approach as in [27] in finding the unoccupied channels of the spectrum, but our introduced WA based on the EGN model is taking into account the nonuniform NLIN distribution, while the exploited OFDM-model in [27] considers a uniform NLIN for all the channels.

In this work, we assume that all network lightpaths can have different launch power values (similar to the assumption introduced in [28], [29]), then the SNR in each WDM channel is expressed as a convex function of these power values. The optimization objective is to maximize the minimum SNR or the network's total AR. The above mentioned EGN model [12] instead of the GN model, capable of including the modulation-format dependency, is exploited to compute the SNR or QoT of network lightpaths. Furthermore, in contrast to the full spectrum utilization assumption in [19], we consider a network with partially utilized links spectrum of links. The results show that a significant gain can be obtained in systems facing multiple SNR requirements due to partial wavelength fill or variable noise spectra, as it was previously conjectured in [26]. A gradient based locally convex optimization approach rather than MILP [5]–[7] is used to mitigate the computational complexity considerably, making it not only applicable to static but also dynamic optical networking. In brief, the main contributions in this work are summarized as follows.

- Proposing joint optimization of RWA and power allocation of coherent optical networks to maximize their total AR and minimum SNR margins by the EGN model for empirically-motivated partially utilized spectrum fiber-optic links.
- Introducing gradient-based locally convex optimization rather than the common MILP methods, resulting in a lower complexity method applicable not only to static but also dynamic optical networking

Finally, numerical network simulations are provided for the Deutsche Telekom Germany (DTG) network, indicating 2.3 dB improvement of the network's minimum SNR margin by multidimensional power optimization compared to flat launch power optimization. Interestingly, it is seen that maximizing the minimum SNR margin is obtained by allocating the highest launch powers to the channels experiencing the highest NLIN efficiency.

The rest of this paper is organized as follows: In Section II, we describe the link nonlinear model based on the EGN model and the exploited network performance metrics are addressed in Section III. In Section IV, we describe the introduced joint routing, wavelength, and power allocation algorithm. Building on this, we look at the numerical results for the DTG network example in Section IV. Finally, Section V concludes this paper by providing some comparisons and benchmarks.

II. Link nonlinear model

To make the paper self-contained, we provide some preliminary information about the channel model, performance metrics, and convexity analysis, necessary in describing the introduced algorithm for joint routing, spectrum, and power allocation. In this work, the EGN model [12] is used to provide a mathematically tractable performance analysis, capable of modeling the dependence of the NLIN on the exploited modulation format and empirically well-validated. This model is obtained for uncompensated optical links with coherent transmission in the quasi-linear regime (with sufficient amount of accumulated chromatic dispersion) [9]. The additive noise is composed of two linear and nonlinear terms, namely the linear amplified spontaneous emission (ASE) noise and the NLIN. More precisely, in a fiber-optic link with N WDM channels, the additive noise variance of channel k is given by

$$\sigma_k^2 = \sigma_{\mathrm{L}_k}^2 + \sigma_{\mathrm{NLI}_k}^2, \tag{1}$$

where $\sigma_{\mathrm{L}_k}^2$ represents the variance of the linear ASE and $\sigma_{\mathrm{NLI}_k}^2$ denotes the NLIN variance of channel k. Partial utilization of network link's spectrum results in considerable reduction of MCI effects. Therefore, one may solely consider the XPM terms and ignore all other terms [9], [10], [30] to obtain the contributed NLIN power on a certain lightpath routed on channel k of the WDM link as

$$\sigma_{\mathrm{NLI}_k}^2 = p_k^3 \chi_{\mathrm{SCI}_k} + \sum_{j=1, j\neq k}^{N} p_k p_j^2 \chi_{\mathrm{XPM}_{j,k}}, \tag{2}$$

where p_k is the launch power of k-th channel and the SCI and XPM nonlinear efficiency factors χ_{SCI_k} and $\chi_{\mathrm{XPM}_{j,k}}$ are computed using (9) and (10) in the Appendix, respectively. We notice here that the NLIN efficiency [19] of channel κ in this paper is referred to $\chi_{\mathrm{SCI}_k} + \sum_{j=1, j\neq k}^{N} \chi_{\mathrm{XPM}_{j,k}}$, derived from (2) assuming equal power for all channels. To compute the total NLIN of the lightpath, one may sum up the contributed NLINs from all the links that the lightpath is routed through.

TABLE I
System parameters

Symbol rate R_s	50 Gbaud
Bit rate per lightpath R_l	200 Gbps
Nonlinear coefficient γ	1.3 $\mathrm{W}^{-1}\mathrm{km}^{-1}$
Attenuation coefficient α	0.2 dB/km
Dispersion coefficient D	16.7 ps/nm/km
Optical center wavelength λ	1550 nm
EDFA noise figure F_n	5 dB
Span length L_s	100 km
WDM channel spacing Δf	50 GHz

III. Network performance metrics

The two well-established performance metrics, namely AR and minimum SNR margin [19], [26], are used as the metrics of the network optimization methods introduced in Section IV. To cope with the computational complexity as well as the convergence speed of the optimization algorithm based on these metrics, particularly for large networks, one may need to convert these metrics to a convex form. To this end, the convexity of the noise power given in (1) needs to be

evaluated with respect to the allocated spectrum (the occupied channel vector) and the corresponding power vector, denoted by $\mathbf{p} = [p_1, p_2, ..., p_M]$, where M refers to the total number of lightpaths for all demands in the given traffic matrix. Since the linear ASE noise (the term $\sigma^2_{\mathrm{L}_k}$ in (1)) is independent of these two vectors, one may solely need to focus on the convexity analysis of the nonlinear part, given in (2). The first and second terms of (2) are posynomial functions of the channel power vector $\mathbf{p}$ [26], [31, Ch. 4]. As the sum of two posynomial functions is also a posynomial function itself, we find that (2) is a posynomial function of $\mathbf{p}$. In other words, the nonlinear noise power is a posynomial function of $\mathbf{p}$, since it is a sum of monomial functions with positive coefficients and real exponents. Although posynomial functions are not convex in their natural forms, these functions can be transformed to convex functions by substituting $e^{\mathbf{y}}$ for $\mathbf{p}$. Hence, (2) is convex in logarithm power variable $\mathbf{y}$. Now since $\sigma^2_k(\mathbf{y})$ is convex in the logarithmic variable $\mathbf{y} = [y_1, ..., y_M]$, the corresponding SNR given by $\mathrm{SNR}_k(\mathbf{y}) = e^{y_k}/\sigma^2_k(e^{\mathbf{y}})$ is log-concave and consequently $\log(\mathrm{SNR}_k) = y_k - \log(\sigma^2_k(e^{\mathbf{y}}))$ is concave [26]. We proceed with the convexity analysis of the above metrics in the following sections.

A. Network AR

Although in general the probability distribution function of the NLIN converges to a non-circular Gaussian distribution based on the central limit theorem [9], it is approximated with a circularly-symmetric Gaussian distribution. Considering a discrete-time channel model with additive white Gaussian noise and mismatched decoding (treating interference as noise) [3], the total AR of a network with M dual-polarized lightpaths in its traffic matrix (the M required lightpaths are found by dividing the bit-rates of the traffic matrix demands by R_l, the bit rate per lightpath, and assuming an all-optical network with no regeneration) is

$$\mathrm{AR}(\mathbf{p}) = 2R_s \sum_{m=1}^{M} \log_2(1 + \mathrm{SNR}_m(\mathbf{p})) \quad \text{[bps]}, \tag{3}$$

where $\mathrm{SNR}_m(\mathbf{p}) = p_m/\sigma^2_m(\mathbf{p})$ is the SNR of lightpath m and σ^2_m denotes the accumulated noise over all the engaged links of lightpath m, including both linear and nonlinear noise terms in (1). Defined in this way, the network AR serves as a lower bound on the sum-rate capacity of the network, achievable using Gaussian modulation for all M lightpaths.

Here, considering the log-concavity of SNR in $\mathbf{y}$ and using the approximation $\mathrm{SNR}_m(\mathbf{p}) + 1 \approx \mathrm{SNR}_m(e^{\mathbf{y}})$ for high SNRs, although the log-concavity is not closed under addition, the network AR can be assumed locally concave provided that a reasonable initial power vector is chosen [26]. Hence, the network AR can be maximized with a low complexity numerical gradient ascent optimization method.

B. Network minimum SNR margin

Since the failure probability of the lightpath with the minimum SNR margin is higher than the other lightpaths of a network, maximizing this minimum SNR margin can guarantee the required network service level agreements. The lightpath SNR margin is expressed as $\mathrm{SNR}_m/\mathrm{SNR}_{\mathrm{req}_m}$, where $\mathrm{SNR}_{\mathrm{req}_m}$ is the required SNR at the receiver input of lightpath m. To exploit a gradient-based method for numerical optimization, we minimize the maximum of the SNR inverse values instead of maximizing the minimum network SNR value. To this end, the network minimum SNR margin can be written as an affine function by exploiting the same change of variable to express the optimization problem as

$$\min\Big(\max_{m\in\{1,...,M\}}\Big(\log(\mathrm{SNR}_{\mathrm{req},m})+\log(\sigma^2_m(e^{\mathbf{y}}))-y_m\Big)\Big). \tag{4}$$

To minimize the maximum of these M posynomial functions, one may consider an upper bound, denoted by s, for all of them and then aim at minimizing this upper bound as

$$\begin{aligned} \min \quad & s \\ \text{s. t.} \quad & \Big(\log(\mathrm{SNR}_{\mathrm{req},m}) + \log(\sigma^2_m(e^{\mathbf{y}})) - y_m - s\Big) \le 0, \\ & m \in \{1, ..., M\}. \end{aligned} \tag{5}$$

Moreover, to obtain an optimization problem with no inequality constraints and apply Newton's method, one can use the indicator function

$$I(u) = \begin{cases} 0 & u \le 0 \\ \infty & u > 0, \end{cases} \tag{6}$$

to get

$$\min\Big[s + \sum_{m=1}^{M} I\Big(\log(\mathrm{SNR}_{\mathrm{req},m}) + \log(\sigma^2_m(e^{\mathbf{y}})) - y_m - s\Big)\Big]. \tag{7}$$

Finally, to make the indicator function twice differentiable, one may use its approximation $\widehat{I}(u) \approx (-1/t)\log(-u)$ [31, Ch. 11], to obtain

$$\min\Big[s - \frac{1}{t}\sum_{m=1}^{M} \log\Big(y_m + s - \log(\mathrm{SNR}_{\mathrm{req},m}) - \log(\sigma^2_m(e^{\mathbf{y}}))\Big)\Big]. \tag{8}$$

We notice that the approximation accuracy of the indicator function is managed by the parameter t such that for high and low accuracy barriers, M/t must be less than 10^{-6} and 10^{-3}, respectively. To this end, one may exploit a sequential unconstrained minimization or barrier method [31, Ch. 11] to solve the problem in a sequence of unconstrained minimization problems such that in each step the resulting point from the previous step is used until M/t becomes less than 10^{-3} or 10^{-6}. In the numerical simulations, we exploit a sequence of increasing values of t until reaching the desired M/t value.

IV. Joint RWA and Power Allocation Algorithm

In this section, we present a physical-layer-aware gradient-based algorithm to perform RWA and power allocation in optical networks with coherent transmission in the quasi-linear regime. Optical networking or network planning is performed based on the two metrics discussed in Section III using the EGN model, briefly discussed in Section II. To realize the joint RWA and power allocation algorithm, we start with finding k candidate lightpaths for each lightpath from the traffic matrix exploiting the Dijkstra k-shortest path algorithm.

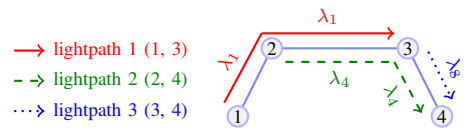

Fig. 1. A simple 4-node WDM network with three lightpaths.

The exploited metric of the Dijkstra algorithm is the minimum NLIN. Since each selected lightpath gets exposed to a different spectrum shape (neighbor wavelengths) at different spans, there may be a lightpath longer than the shortest lightpath selected by the Dijkstra algorithm, but experiencing a lower nonlinear inter-channel interference, leading to a smaller NLIN power in the received signal introduced in (2). The main reason causing a higher NLIN power in a shorter lightpath is the denser occupied spectrum in some links of the lightpath, therefore the longer path is preferred in this case.

Taking into account the selected k shortest lightpaths, we exploit a similar approach as in [27], to fulfill the spectrum continuity condition in the wavelength assignment process (i.e., the same wavelength index needs to be used for all the links of each lightpath). Here, we describe the wavelength allocation of the k candidate lightpaths, starting from a source node, traversing transparently through several links, eventually ending at the destination node.

To this end, we define the occupied channel vector (OCV) of a link whose elements correspond to the occupied wavelength indices, e.g., the OCV of link ℓ between nodes i and j, denoted by OCV_ℓ or $\text{OCV}_{(i,j)}$ is the vector $\{\lambda_2, \lambda_7, \lambda_{10}\}$, representing that the occupied channels in this link are located at wavelengths λ_2, λ_7, and λ_{10}. We also denote the complement of the OCV as the unoccupied channel vector (UCV) of the link. One may readily define the OCV of a lighpath as the union of the OCVs of involved links in the lighpath. As an example, Fig. 1 shows a simple 4-node WDM network with eight exploited wavelengths. For the shown lightpaths 1, 2, and 3 with the (source, destination) pairs of (1,3), (2,4), and (3,4), respectively, the OCVs of this network links are given as $\text{OCV}_{(1,2)} = \{\lambda_1\}$, $\text{OCV}_{(2,3)} = \{\lambda_1, \lambda_4\}$, $\text{OCV}_{(3,4)} = \{\lambda_4, \lambda_8\}$. Consequently, the OCV and UCV of the lightpath between nodes 1 and 4 are computed as $\text{OCV}_{(1,4)} = \text{OCV}_{(1,2)} \cup \text{OCV}_{(2,3)} \cup \text{OCV}_{(3,4)} = \{\lambda_1, \lambda_4, \lambda_8\}$ and $\text{UCV}_{(1,4)} = \{\lambda_1, \lambda_2, ..., \lambda_8\} - \text{OCV}_{(1,4)} = \{\lambda_2, \lambda_3, \lambda_5, \lambda_6, \lambda_7\}$.

The joint RWA and power allocation algorithm is carried out after sorting the demands of the given traffic matrix based on their bit-rates in descending order, considering the same assumption as [32], [33]. As seen in line 1 of Algorithm 1, the demands with higher rates will have higher priorities in the resource (routing, wavelength, and power) allocation process. Therefore, one may conclude that the solution of Algorithm 1 is independent of the order of demands appearing in the traffic matrix.

To jointly choose a wavelength for path j with L links from its UCV and optimize the optical launch powers of the lightpaths for a given traffic matrix (i.e., static network planning), we continue with the previously selected k candidate lightpaths. As summarized in the Joint Optimization Algorithm pseudo-code in Algorithm 1, for each candidate path, we assign the first element of its UCV as a temporary wavelength to path j (addressed in line 8 of Algorithm 1) and by grouping this path and the previously established lightpaths (up to this step) together (addressed in line 9 of Algorithm 1) and running the convex optimization algorithm with the objective of maximizing the network AR or minimum SNR margin, described in Sections III-A and III-B, respectively, we find the i-dimensional optimum power vector (or an optimum flat launch power) of the group (addressed in line 10 of Algorithm 1). Then, we move on with the next element of the UCV until we have the relevant metric values computed for all the UCV elements. The wavelength resulting in the highest network AR or minimum SNR margin values (addressed in line 14 of Algorithm 1) is selected for the corresponding candidate path. We perform this procedure for all the k candidate paths. Among these candidate paths, the one which results in the highest metrics is selected and assign to lightpath i (addressed in line 17 of Algorithm 1). This procedure is performed iteratively until all the demands are given the required resources: route, wavelength, and launch power.

Algorithm 1: Joint Optimization Algorithm

Input : Traffic matrix and network topology
Output: The route, wavelength and launch power of all the lightpaths in the traffic matrix

1 Sort the demands in the traffic matrix based on their bit-rates, in descending order (higher priorities for demands with higher rates)
2 Divide the bit-rates of the traffic matrix demands by R_l to find the number of the required lightpaths for each demand, and denote their sum by M
3 **for** $i = 1, \ldots, M$ **do**
4 Find k shortest candidate paths for lightpath i
5 **for** $j = 1, \ldots, k$ **do**
6 **for** $\omega = 1, \ldots, N$ **do**
7 **if** $\lambda_\omega \in UCV_j$ **then**
8 Assign wavelength ω to path j
9 Make a group of i lightpaths, consisting of the previous $i-1$ lightpaths together with path j
10 i-dimensional or flat power optimization within the group
11 Store the metric value and wavelength
12 **end**
13 **end**
14 Select the wavelength with the best metric value
15 Store the metric value and wavelength
16 **end**
17 Select lightpath i among the k candidates with the best metric value
18 **end**

V. Numerical Results

Numerical simulations are provided in this section to evaluate the presented network planning algorithm based on the

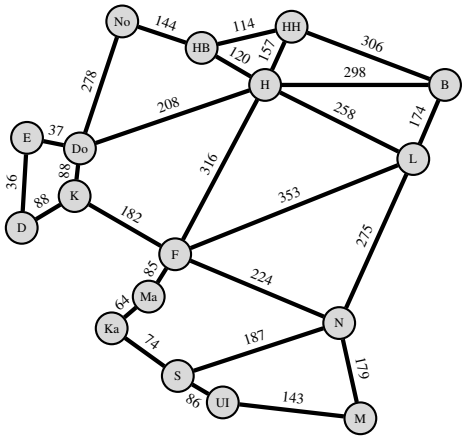

Fig. 2. The DTG network with 17 nodes and 26 links. The numbers on the links indicate the length in km.

two metrics discussed in Section III for the DTG national scale network, depicted in Fig. 2. Here, we assume that the links are capable of accommodating 87 Nyquist channels with WDM channel spacing of 50 GHz (as noted in Table I, $R_s = \Delta f$). The lengths (in km) are tagged to the links in the drawn network topology. The traffic matrix is generated using the voice and data traffic estimation provided in [34] for different network topologies. It is assumed that each channel is capable of carrying a data rate of R_l; therefore one may obtain the required number of wavelengths for each traffic matrix demand (overall $M = 122$ lightpaths for this numerical simulation) by dividing its data rate by R_l. We assume all lightpaths experience the highest NLIN for flat power optimization, which is the same assumption as in [19], [26].

A. Maximizing the network AR

The simulations are carried out with polarization multiplexed quadrature phase shift keying (PM-QPSK) as well as Gaussian modulation and the numerical results in the first row of Fig. 3 show the SNR of each lightpath after M-dimensional and flat launch power optimization. As shown in these figures, the SNRs improve when the Joint Optimization Algorithm with M-dimensional power optimization is conducted, compared to flat power optimization. Using (3), the network AR for Gaussian modulation with M-dimensional power optimization is about 85 Tbps, compared to 72.5 Tbps for flat power optimization, giving rise to about 17% network AR improvement. As these figures indicate, the SNR values of the lightpaths degrade for Gaussian modulation, since the Φ_k and Ψ_k values given in (15) are equal to zero for this format, whereas for PM-QPSK, theses coefficients get negative values.

B. Maximizing the network minimum lightpath SNR margin

Analogously to the previous section, the proposed algorithm based on maximizing the minimum lightpath SNR is evaluated with M-dimensional and flat power optimization in the second row of Fig. 3. As seen in these figures, the minimum SNR is improved remarkably by using M-dimensional power optimization compared to flat power optimization for PM-QPSK and polarization multiplexed 16 ary quadrature amplitude modulation (PM-16QAM). According to the numerical simulation shown in Fig. 3, the minimum SNR margin improvement is about 2.4 dB and 2.3 dB for PM-QPSK and PM-16QAM, respectively (the solid arrows show the margin improvement, drawn between the minimum SNR margin values of the two curves). Moreover, the numerical results in the second row of Fig. 3 indicate that the majority of lightpaths get allocated the same SNR values after M-dimensional power optimization, interpreted as smoothing the SNR values resulting from flat launch power optimization to push up and down their minimum and maximum SNR values, respectively.

Fig. 4 shows the NLIN power of lightpaths as well as their launch powers. This figure indicates that the launch powers are following the same power density distribution as the NLIN power. It can be intuitively concluded that the lightpath experiencing the lowest NLIN efficiency must be launched with the lowest transmit power to maximize the minimum SNR of the lightpaths. In other words, lightpaths traversing a longer routing path distance, especially those exposed to a large number of neighbors in the traversed links, need to be launched with a higher transmit power.

C. Complexity

Since the computational complexity of the gradient calculations in the proposed algorithm grows with the total number of lightpaths, the computational complexity of maximizing the network AR increases with increasing traffic matrix size. On the other hand, the computational complexity of SNR margin optimization is much higher than AR optimization, resulting from exploiting a barrier optimization method. To evaluate the computational complexity of Algorithm 1, we compute the run time of the most time-consuming part of the algorithm (finding the optimum launch power vector) as a complexity criterion. As shown in Fig. 5, by considering the numerical run time on a certain platform (an Intel Core i7-4702MQ 2.2 GHz processor with 8 GB RAM) and MATLAB simulation on Windows 8.1), it is found empirically that the computational complexity of SNR margin optimization grows near-quadratically with respect to the number of lightpaths, whereas the complexity of network AR optimization grows slower.

One may approximate the EGN model in a linear form to reduce the computation complexity of both algorithms. However, the computational complexity of joint power allocation and RWA optimization using MILP still remains NP-complete [28].

VI. Discussion and conclusion

We presented a QoT-aware convex formulated network optimization by exploiting a closed-form channel model, accurately explaining the influence of wavelength, routing, and power allocation on the QoT of optical networks lightpaths. To this end, a joint routing, wavelength, and power allocation algorithm was proposed using the EGN model for optical coherent networks with partial link spectrum utilization. Two criteria are exploited in network optimization, namely maximizing the network AR and minimizing the SNR margin. The performance of the algorithm was evaluated using extensive numerical simulations on the DTG network, indicating a margin gain of 2.3 dB on average using this joint optimization

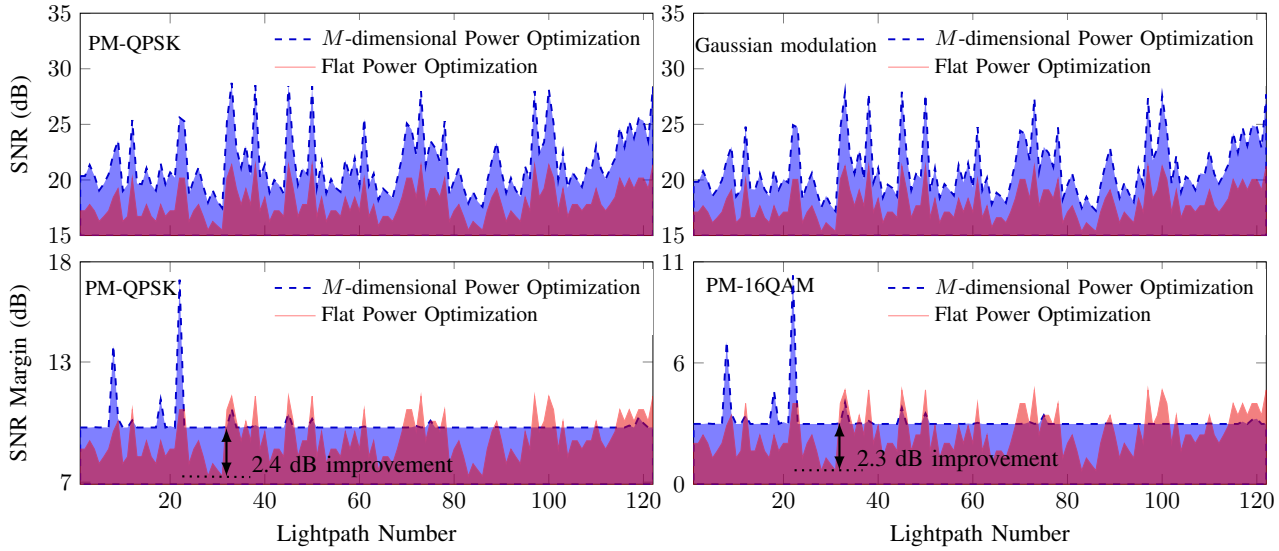

Fig. 3. The optimized SNRs of the simulated network lightpaths by the Joint Optimization Algorithm with M-dimensional and flat launch power based on maximizing the network AR (first row) and the optimized SNR margins based on maximizing the minimum SNR margin (second row).

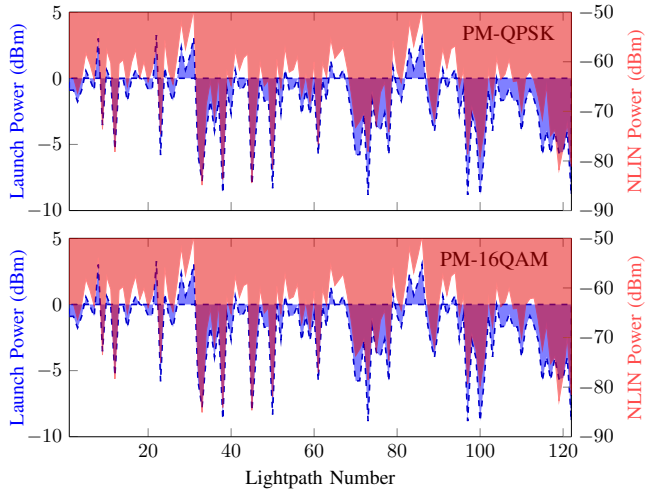

Fig. 4. The optimized launch (dashed curves) and NLIN (solid curves) power values by M-dimensional optimization based on maximizing the minimum SNR margin for the PM-QPSK and PM-16QAM modulation formats.

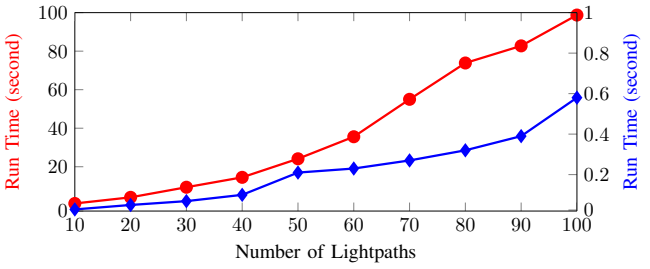

Fig. 5. The run time of Algorithm 1 for finding the optimum launch power vector based on maximizing the network AR (blue diamond) or the minimum SNR margin (red circle).

with individual power values for different lightpaths (multi-dimensional) compared to an optimized flat (equal) power for all lightpaths.

Appendix

In this Appendix, the required formulas based on the EGN model are provided to compute χ_{SCI_k} and $\chi_{\text{XPM}_{j,k}}$ for a WDM link defined in Sec. II. The same rectangular Nyquist pulse spectral shape $S(f)$ is assumed for all the WDM channels with the bandwidth of R_s, centered at $f = 0$. As mentioned in Sec. II, we consider just SCI and the dominant terms of the XCI effects, i.e., XPM. The power of SCI and XPM nonlinear effects can be expressed as [12]

$$\chi_{\text{SCI}_k} = D(k,k,k)+\Phi_k(\eta(k,k,k)+\eta'(k,k,k))+\Psi_k\eta''(k,k,k), \tag{9}$$

and

$$\chi_{\text{XPM}_{j,k}} = 2D(k,j,k) + \Phi_j\eta(k,j,k), \tag{10}$$

respectively, where the GN-model term is given by

$$\begin{aligned} D(k_1,k_2,k) = \frac{16}{27}R_s^3 \int_{-R_s/2}^{R_s/2} df \int_{-R_s/2}^{R_s/2} df_1 \int_{-R_s/2}^{R_s/2} df_2 \\ \cdot |S(f_1)|^2|S(f_2)|^2|S(f_1+f_2-f)|^2 \\ \cdot |\mu(f_1+k_1\Delta f, f_2+k_2\Delta f, f+k\Delta f)|^2, \end{aligned} \tag{11}$$

in which

$$\mu(f_1,f_2,f) = \zeta(f_1,f_2,f)\nu(f_1,f_2,f), \tag{12}$$

is the link function [12],

$$\zeta(f_1,f_2,f) = \gamma\frac{1-e^{-2\alpha L_s}e^{j4\pi^2\beta_2(f_1-f)(f_2-f)L_s}}{2\alpha - j4\pi^2\beta_2(f_1-f)(f_2-f)}, \tag{13}$$

indicates the strength of the FWM efficiency, and

$$\begin{aligned} \nu(f_1,f_2,f) = &\frac{\sin\left(2\beta_2\pi^2(f_1-f)(f_2-f)N_sL_s\right)}{\sin\left(2\beta_2\pi^2(f_1-f)(f_2-f)L_s\right)} \\ &\cdot e^{2\beta_2\pi^2(f_1-f)(f_2-f)(N_s-1)L_s}, \end{aligned} \tag{14}$$

represents the coherent addition of NLIN at the receiver. The terms addressing the EGN model non-Gaussianity assumption correction, introduced in (9) and (10), are given as

$$\Phi_k = \frac{\mathbb{E}\{|b_k|^4\}}{\mathbb{E}^2\{|b_k|^2\}} - 2, \quad \Psi_k = \frac{\mathbb{E}\{|b_k|^6\}}{\mathbb{E}^3\{|b_k|^2\}} - 9\frac{\mathbb{E}\{|b_k|^4\}}{\mathbb{E}^2\{|b_k|^2\}} + 12, \tag{15}$$

where $\mathbb{E}$ denotes the expectation operator and b_k denotes the random symbol transmitted over channel k, and

$$\eta(k_1,k_2,k) = \frac{80}{81}R_s^2 \int_{-R_s/2}^{R_s/2} df \int_{-R_s/2}^{R_s/2} df_1 \int_{-R_s/2}^{R_s/2} df_2 \cdot \int_{-R_s/2}^{R_s/2} df_2' |S(f_1)|^2 S(f_2) S^*(f_2') S^*(f_1+f_2-f) \cdot S(f_1+f_2'-f)\mu(f_1+k_1\Delta f, f_2+k_2\Delta f, f+k\Delta f) \cdot \mu^*(f_1+k_1\Delta f, f_2'+k_2\Delta f, f+k\Delta f),$$

$$\eta'(k_1,k_2,k) = \frac{16}{81}R_s^2 \int_{-R_s/2}^{R_s/2} df \int_{-R_s/2}^{R_s/2} df_1 \int_{-R_s/2}^{R_s/2} df_2 \cdot \int_{-R_s/2}^{R_s/2} df_2' |S(f_1+f_2-f)|^2 S(f_1) S(f_2) S^*(f_2') \cdot S^*(f_1+f_2-f_2')\mu(f_1+k_1\Delta f, f_2+k_2\Delta f, f+k\Delta f) \cdot \mu^*(f_1+f_2-f_2'+k_1\Delta f, f_2'+k_2\Delta f, f+k\Delta f),$$

and

$$\eta''(k_1,k_2,k) = \frac{16}{81}R_s \int_{-R_s/2}^{R_s/2} df \int_{-R_s/2}^{R_s/2} df_1 \int_{-R_s/2}^{R_s/2} df_2 \int_{-R_s/2}^{R_s/2} \cdot df_1' \int_{-R_s/2}^{R_s/2} df_2' S(f_1) S(f_2) S^*(f_1') S^*(f_2') S^*(f_1+f_2-f) \cdot S(f_1'+f_2'-f)\mu(f_1+k_1\Delta f, f_2+k_2\Delta f, f+k\Delta f) \cdot \mu^*(f_1'+k_1\Delta f, f_2'+k_2\Delta f, f+k\Delta f),$$

where "*" denotes the complex conjugate operator. The multi-dimensional integrals were evaluated through Monte-Carlo integration [35].

REFERENCES

[1] A. Chralyvy, "Plenary paper: The coming capacity crunch," in *Proc. European Conf. and Exhibition on Optic. Commun.*, Sep. 2009.

[2] R.-J. Essiambre *et al.*, "Capacity limits of optical fiber networks," *J. Lightwave Technol.*, vol. 28, no. 4, pp. 662–701, Feb. 2010.

[3] M. Secondini and E. Forestieri, "Scope and limitations of the nonlinear Shannon limit," *J. Lightwave Technol.*, vol. 35, no. 4, pp. 893–902, Apr. 2017.

[4] S. J. Savory, "Congestion aware routing in nonlinear elastic optical networks," *IEEE Photon. Technol. Lett.*, vol. 26, no. 10, pp. 1057–1060, May 2014.

[5] X. Wan, N. Hua, and X. Zheng, "Dynamic routing and spectrum assignment in spectrum-flexible transparent optical networks," vol. 4, no. 8, pp. 603–613, Aug. 2012.

[6] M. Klinkowski and K. Walkowiak, "Routing and spectrum assignment in spectrum sliced elastic optical path network," *IEEE Commun. Lett.*, vol. 15, no. 8, pp. 884–886, Aug. 2011.

[7] K. Christodoulopoulos, I. Tomkos, and E. Varvarigos, "Elastic bandwidth allocation in flexible OFDM-based optical networks," *J. Lightwave Technol.*, vol. 29, no. 9, pp. 1354–1366, May 2011.

[8] J. Zhao, H. Wymeersch, and E. Agrell, "Nonlinear impairment-aware static resource allocation in elastic optical networks," *J. Lightwave Technol.*, vol. 33, no. 22, pp. 4554–4564, Nov. 2015.

[9] A. Mecozzi and R. J. Essiambre, "Nonlinear Shannon limit in pseudolinear coherent systems," *J. Lightwave Technol.*, vol. 30, no. 12, pp. 2011–2024, Jun. 2012.

[10] R. Dar *et al.*, "Properties of nonlinear noise in long, dispersion-uncompensated fiber links," *Opt. Express*, vol. 21, no. 22, pp. 25 685–25 699, Nov. 2013.

[11] P. Poggiolini, "The GN model of non-linear propagation in uncompensated coherent optical systems," *J. Lightwave Technol.*, vol. 30, no. 24, pp. 3857–3879, Dec. 2012.

[12] A. Carena *et al.*, "EGN model of non-linear fiber propagation," *Opt. Express*, vol. 22, no. 13, pp. 16 335–16 362, Jun. 2014.

[13] P. Johannisson and M. Karlsson, "Perturbation analysis of nonlinear propagation in a strongly dispersive optical communication system," *J. Lightwave Technol.*, vol. 31, no. 8, pp. 1273–1282, Apr. 2013.

[14] R. Dar *et al.*, "Accumulation of nonlinear interference noise in fiber-optic systems," *Opt. Express*, vol. 22, no. 12, pp. 14 199–14 211, Jun. 2014.

[15] M. Secondini, E. Forestieri, and G. Prati, "Achievable information rate in nonlinear WDM fiber-optic systems with arbitrary modulation formats and dispersion maps," *J. Lightwave Technol.*, vol. 31, no. 23, pp. 3839–3852, Dec. 2013.

[16] M. Jinno *et al.*, "Distance-adaptive spectrum resource allocation in spectrum-sliced elastic optical path network [topics in optical communications]," *IEEE Commun. Mag.*, vol. 48, no. 8, Aug. 2010.

[17] Y. Li *et al.*, "Adaptive FEC selection for lightpaths in elastic optical networks," *in Proc. Optic. Fiber Commun. Conf.*, pp. W3A–7, 2014.

[18] ——, "Adaptive FEC-based lightpath routing and wavelength assignment in WDM optical networks," *Optical Switching and Networking*, vol. 14, pp. 241–249, Aug. 2014.

[19] D. Ives *et al.*, "Adapting transmitter power and modulation format to improve optical network performance utilizing the Gaussian noise model of nonlinear impairments," *J. Lightwave Technol.*, vol. 32, no. 21, pp. 4087–4096, Nov. 2014.

[20] L. Beygi *et al.*, "A discrete-time model for uncompensated single-channel fiber-optical links," *IEEE Trans. Commun.*, vol. 60, no. 11, pp. 3440–3450, Nov. 2012.

[21] A. Carena *et al.*, "Modeling of the impact of nonlinear propagation effects in uncompensated optical coherent transmission links," *J. Lightwave Technol.*, vol. 30, no. 10, pp. 1524–1539, May 2012.

[22] P. Johannisson and E. Agrell, "Modeling of nonlinear signal distortion in fiber-optic networks," *J. Lightwave Technol.*, vol. 32, no. 23, pp. 4544–4552, Dec. 2014.

[23] P. Poggiolini *et al.*, "The GN-model of fiber non-linear propagation and its applications," *J. Lightwave Technol.*, vol. 32, no. 4, pp. 694–721, Feb. 2014.

[24] D. A. A. Mello *et al.*, "Optical networking with variable-code-rate transceivers," *J. Lightwave Technol.*, vol. 32, no. 2, pp. 257–266, Jan. 2014.

[25] D. J. Ives, P. Bayvel, and S. J. Savory, "Routing, modulation, spectrum and launch power assignment to maximize the traffic throughput of a nonlinear optical mesh network," *Photonic Network Communications*, vol. 29, no. 3, pp. 244–256, Jun. 2015.

[26] I. Roberts, J. M. Kahn, and D. Boertjes, "Convex channel power optimization in nonlinear WDM systems using Gaussian noise model," *J. Lightwave Technol.*, vol. 34, no. 13, pp. 3212–3222, Jul. 2016.

[27] H. Beyranvand and J. A. Salehi, "A quality-of-transmission aware dynamic routing and spectrum assignment scheme for future elastic optical networks," *J. Lightwave Technol.*, vol. 31, no. 18, pp. 3043–3054, Sep. 2013.

[28] L. Yan *et al.*, "Joint assignment of power, routing, and spectrum in static flexible-grid networks," *J. Lightwave Technol.*, vol. 35, no. 10, pp. 1766–1774, May 2017.

[29] ——, "Resource allocation for flexible-grid optical networks with nonlinear channel model," vol. 7, no. 11, pp. B101–B108, Nov. 2015.

[30] P. Poggiolini *et al.*, "Analytical and experimental results on system maximum reach increase through symbol rate optimization," *J. Lightwave Technol.*, vol. 34, no. 8, pp. 1872–1885, Apr. 2016.

[31] S. Boyd and L. Vandenberghe, *Convex Optimization*. New York: Cambridge University Press, 2004.

[32] F. Dikbiyik, M. Tornatore, and B. Mukherjee, "Minimizing the risk from disaster failures in optical backbone networks," *J. Lightwave Technol.*, vol. 32, no. 18, pp. 3175–3183, Sep. 2014.

[33] M. Batayneh *et al.*, "On routing and transmission-range determination of multi-bit-rate signals over mixed-line-rate WDM optical networks for carrier ethernet," *IEEE/ACM Trans. Networking*, vol. 19, no. 5, pp. 1304–1316, Oct. 2011.

[34] A. Betker *et al.*, "Reference transport network scenarios," *MultiTeraNet Report, July*, 2003.

[35] R. E. Caflisch, "Monte Carlo and quasi-Monte Carlo methods," *Acta numerica*, vol. 7, pp. 1–49, 1998.